HHS Public Access

Author manuscript

J Orthop Res. Author manuscript; available in PMC 2018 April 01.

Published in final edited form as:

J Orthop Res. 2017 April ; 35(4): 868–875. doi:10.1002/jor.23332.

In Vivo Visualization Using MRI T_2 Mapping of Induced Osteochondrosis and Osteochondritis Dissecans Lesions in Goats Undergoing Controlled Exercise

Ferenc Tóth[1], **Frédéric H. David**[2], **Elizabeth LaFond**[2], **Luning Wang**[3], **Jutta M. Ellermann**[3], and **Cathy S. Carlson**[1]

[1]Veterinary Population Medicine Department, University of Minnesota, St. Paul, MN, USA

[2]Veterinary Clinical Sciences Department, University of Minnesota, St. Paul, MN, USA

[3]Center for Magnetic Resonance Research, Department of Radiology, University of Minnesota, Minneapolis, MN, USA

Abstract

In vivo visualization of subclinical osteochondrosis(OC) lesions, characterized by necrosis of epiphyseal growth cartilage, is necessary to clarify the pathogenesis of this disease. Hence, our objectives were to demonstrate induced necrosis of the epiphyseal cartilage *in vivo* using MRI and to monitor progression or resolution of resulting lesions. We also aimed to improve the goat model of OC by introducing controlled exercise. Vascular supply to the epiphyseal cartilage was surgically interrupted in four 5-day-old goats to induce ischemic cartilage necrosis in a medial femoral condyle. Starting 3 weeks postoperatively, goats underwent daily controlled exercise until euthanasia at 6, 10, 11 (n=2) weeks postoperatively. T_2 maps of operated and control femora were obtained *in vivo* at 3(n=4), 6(n=4), 9(n=3) and 11(n=2) weeks postoperatively using a 3T MR scanner. *In vivo* MRI findings were validated against MRI results obtained *ex vivo* at 9.4T in three goats and compared to histological results in all goats. Surgical interruption of the vascular supply caused ischemic cartilage necrosis in 3 out of 4 goats. T_2 maps obtained *in vivo* at 3T identified regions of increased relaxation time consistent with discrete areas of cartilage necrosis 3 to 11 weeks postoperatively and demonstrated delayed progression of the ossification front at 9(n=1) and 11(n=2) weeks postoperatively. *In vivo* MRI findings were confirmed by *ex vivo* MRI at 9.4T and by histology. Identification of cartilage necrosis in clinical patients in the early stages of OC using T_2 maps may provide valuable insight into the pathogenesis of this condition.

Keywords

cartilage necrosis; T_2 map; MRI; osteochondrosis; osteochondritis dissecans

Corresponding author: Ferenc Tóth, Department of Veterinary Population Medicine, College of Veterinary Medicine, University of Minnesota; 435 AnSci/VetMed, 1988 Fitch Avenue, St. Paul, MN 55108, USA; ftoth@umn.edu; Tel.: 612-624-7727.

Author contribution: The study was designed by FT and CSC with critical input from JME, FHD, EL and LW. Data collection, processing and analysis were performed by FT, FHD, LW, EL, JME and CSC. The manuscript was primarily written by FT and CSC and was critically revised by FHD, LW, EL and JME. All authors have approved the final, submitted version of the manuscript.

Introduction

Osteochondrosis (**OC**) is a developmental orthopaedic disease that affects humans and various animal species (1; 2). The clinically apparent form of the disease is called osteochondrosis dissecans (veterinary medicine) or osteochondritis dissecans **(OCD**, human medicine), and is characterized by intra articular formation of (osteo)chondral flaps or fragments that, if left untreated, can trigger the development of osteoarthritis (3; 4).

Histological studies performed on specimens obtained from asymptomatic animals, along with proof-of-principle studies utilizing surgical interruption of the vascular supply to a well defined portion of the articular-epiphyseal cartilage complex (**AECC**), not only revealed the existence of subclinical OC in various animal species but also provided critical information on the role of ischemia in its pathogenesis (5–8). Focal, ischemic necrosis of the epiphyseal cartilage, uniformly associated with necrotic cartilage canal vessels, was demonstrated to be the earliest change associated with subclinical OC (9). Until very recently, visualization of this clinically silent lesion was only possible using histological techniques, therefore it is termed OC latens. With progression of the disease, conversion of necrotic cartilage islands to bone is delayed, leading to focal failure of enchondral ossification. At this point, lesions become radiographically evident as depressions in the subchondral bone and they are termed OC manifesta. It is purported that, eventually, biomechanical stress imposed over articular cartilage inadequately supported by subjacent necrotic epiphyseal cartilage causes clefting, resulting in clinically apparent OCD (2).

Unfortunately, similar studies of subclinical OC are not possible in human beings because of their invasive nature and the lack of adequate numbers of cadaveric specimens. Hence, the existence of subclinical OC latens lesions has not been described in human subjects, and lesions resembling to OC manifesta are often considered to be normal ossification variants (10; 11). This leaves the pathogenesis of human OC to be undetermined, with several competing theories promoted (12). It is expected that better understanding of human OC will only stem from the development of novel, non-invasive, *in vivo* imaging modalities which have the ability to identify early cartilage necrosis/ischemia.

Recently, development and validation of novel MRI sequences led to an increased interest in advanced cartilage imaging (13–15). Quantitative MRI techniques, including cartilage maps created using T_2 –, RAFF (relaxation along a fictitious field) –, or $T_{1\rho}$ – relaxation times, were able to identify surgically-induced, subclinical lesions of OC *ex vivo* at various stages in their temporal development (16). Susceptibility weighted imaging and quantitative susceptibility mapping (17; 18) have also been used to describe the vascular architecture of the epiphyseal growth cartilage at the distal femoral predilection site of OC in human beings, pigs, horses, and goats *ex vivo* (19; 20). The goat model of induced cartilage necrosis has been used in several studies (16; 21; 22), in spite of its known shortcoming that induced subclinical OC lesions to date have failed to progress to OCD in the operated goats. Nevertheless, *in vivo* translation of these *ex vivo* MRI studies to a clinically relevant field strength should be completed before they can be applied in human patients afflicted with (subclinical) OC.

To address the shortcomings of the goat model of OC and to evaluate the *in vivo* applicability of the above mentioned MRI techniques, the primary objectives of the present study were to (1) utilize a controlled exercise training program to facilitate progression of OC manifesta lesions to OCD in the goat model, (2) demonstrate surgically induced ischemic cartilage necrosis in this model *in vivo* using MRI at a clinically relevant field strength, and (3) monitor progression or healing of cartilage necrosis over time. We hypothesized that controlled exercise instituted after interruption of the blood supply to the distal femoral epiphyseal cartilage would facilitate the development of OCD in the goat model, and that T_2 cartilage maps obtained *in vivo* would allow detection and monitoring of subclinical OC lesions.

Materials and Methods

Animals

The study design and all procedures were approved by the University of Minnesota Institutional Animal Care and Use Committee (IACUC # 1504-32501A). Using a technique described in detail previously (21), four 5-day-old male goat kids received surgery to interrupt the vascular supply to the AECC of the axial aspect of the medial femoral condyle (**MFC**) in the right pelvic limb. In each animal, the left pelvic limb served as an unoperated control. Briefly, the goats were placed under general anesthesia using isoflurane vaporized in oxygen and the right pelvic limb was prepared for aseptic surgery. The stifle joint was approached using a lateral parapatellar arthrotomy, which allowed medial luxation of the patella exposing the intercondylar grove and the axial aspect of the medial femoral condyle. A custom-made 5 × 5 mm blade was used to create an incision extending into the AECC of the axial aspect of the MFC, parallel with the articular surface (21). The joint capsule and the subcutaneous tissues were closed separately using 3-0 polydioxanon in a simple continuous pattern. The skin was apposed using intradermal sutures using the same suture material and pattern. Postoperatively, the goats received an antimicrobial drug (ceftiofur 2.2 mg/kg IM, twice daily) and analgesic treatment (flunixin meglumine 1.1 mg/kg SC, twice daily) for 3 days, and remained confined to an approximately 9 × 12 feet stall for 7 days with a light bandage applied to the surgical site. Three weeks postoperatively the goats were entered into a controlled exercise program, including a regimen of joint concussive activity, for 20 minutes once/day for 5 days/week. Specifically, goats were run on the land treadmill at 2–5 mph for 10 minutes (speed increased towards the end of the study as the goats became more accustomed to running on the treadmill) and were subsequently directed through an obstacle course at a brisk trot for an additional 10 minutes. The obstacle course included a dog agility A-frame and 5 shoulder-height jumps. Food motivation and encouragement were successfully used to maintain activity. Over the course of the study, goats received *in vivo* MRI examinations at 3 (n=4), 6 (n=4), 9 (n=3) and 11 (n=2) weeks postoperatively (Table 1). Three of the goats were euthanized at 6 (n=1) and 11 (n=2) weeks postoperatively, immediately after completion of the *in vivo* MRI studies. The remaining goat was euthanized 10 weeks postoperatively (1 week after completion of the 9 week MRI). Immediately after euthanasia, distal femora were harvested bilaterally and imaged *ex vivo* in 3 out of 4 goats using an ultra high field (9.4 T) MRI scanner. Logistical difficulties did not allow for *ex vivo* 9.4T MRI of the specimen obtained from the goat euthanized 6 weeks

postoperatively. Upon conclusion of the *ex vivo* imaging, distal femora were fixed in 10% neutral buffered formalin for 48h.

In vivo* MRI—In vivo* MRI was performed on goats anesthetized with isoflurane vaporized in oxygen in a 3 Tesla clinical scanner (GE Signa Excite, Milwaukee, WI, USA) using a quadrature transmit/receive wrist coil (Mayo Clinic BC-10). Goats were positioned in dorsal recumbency with the pelvic limbs extended and each pelvic limb was scanned separately, starting with the right side. The wrist coil was positioned with its isocenter at the level of the femorotibial joint. Foam pads were inserted in the coil to maintain the femoral condyles in the isocenter of the coil. Two-dimensional Proton Density (PD) - weighted Fast Spin Echo (FSE) images (TR = 1667–1684 ms, TE = 42 ms, echo train length [ETL] = 10, matrix = 256 × 256, field-of-view [FOV] = 10 cm × 10 cm, slice thickness = 2 mm, 15–19 interleaved slices) were obtained in the axial (number of excitation [NEX] = 2, spacing = 0.6 mm), coronal (NEX = 6, spacing = 0.6 mm) and sagittal (NEX = 6, spacing = 0.2 mm) planes. Quantitative T_2-mapping was acquired using a Multi-Echo–Spin Echo sequence (TR = 1000 ms, TEs = 8, 17, 25, 33, 41, 50, 58 and 66 ms, Matrix = 256 × 256, FOV = 8 cm × 8cm, slice thickness = 2 mm, spacing = 0.4 mm, 6 interleaved slices) in the sagittal (NEX = 3) and coronal (NEX = 4) planes. The total scan time was approximately one hour per limb. Color-coded T_2 maps were generated using commercially available software (Cartigram, GE Medical Systems, Milwaukee, WI, USA) with a log-linear least square exponential fit model. Regions of interest (ROI) were manually selected by a veterinary radiologist (FHD). The slice for the ROI of the operated limb was selected in the coronal plane utilizing the gray scale first echo image (8ms) obtained from the multiecho Spin Echo sequence. The sagittal PD-weighted images and coronal images were co-referenced to determine the slice closest to the surgical incision. For the control leg, a slice of similar location was selected based on anatomical references (the slice intersecting with the same level in the physeal lines and medial meniscus, based on the sagittal images). Once the slices were determined, an oval ROI of $2mm^2$ in the medial femoral condyle epiphyseal cartilage was selected with its most axial (central) edge placed 1.5 mm abaxial (lateral) from the axial (central) limit of the visible cartilage. The operator was blinded to the T_2 color maps, when identifying the ROI's.

Ex vivo* MRI—Ex vivo* MRI of the distal femora was conducted in a 9.4 Tesla small animal MRI scanner (Agilent Technologies, Santa Clara, CA, USA). A shielded quadrature volume coil (Millipede, Varian NMR Systems, Palo Alto, CA) was used for both RF transmission and signal acquisition. Distal femoral specimens were placed into a latex container and immersed in perfluoropolyether oil for a proton-clean and susceptibility-matched background. A 2D – FSE sequence with different magnetization preparations was implemented to measure T_2 (double spin echo preparation, TE = 4, 20, 40, 60, 80, and 100 ms), and adiabatic $T_{1\rho}$ (Train of 0, 4, 8, 12, 16 hyperbolic secant (HS4) pulses, duration = 6 ms, γB_1^{max} = 2.5 kHz) relaxation times (16). The parameters of the FSE sequence were as follows: TR/TE = 5 s / 5.38 ms, ETL = 8, matrix = 256 × 256, one coronal slice = 1 mm, acquisition bandwidth = 131.6 kHz, FOV = 4.3 cm × 4.3 cm. To improve the accuracy of the MRI experiment, B_0 field shimming and B_1 calibration were performed before the FSE sequences.

Histology—Formalin fixed distal femora were decalcified by immersion in EDTA for 2–4 weeks. Femoral condyles were subsequently trimmed in the coronal plane into approximately 3 mm thick slabs, which were embedded into paraffin blocks and routinely processed for histology. Five μm thick sections were cut from the surface of each block and were stained using hematoxylin and eosin. Selected blocks were serially sectioned until sections matching the locations of the *in vivo* T_2 maps were identified based on anatomical landmarks and the presence of the surgical scar. Sections stained with safranin O were used to validate MRI findings by demonstrating changes characteristic of ischemic cartilage necrosis (chondrocyte cell death accompanied by pallor of the extracellular matrix).

Results

All surgical procedures were completed without any complications. In the postoperative period one goat (Goat 1, see Tables 1 and 2) developed a superficial incisional surgical site infection, which was treated with debridement and sterile saline lavage until its resolution 6 weeks postoperatively. The exercise-training regimen was successfully implemented in all 4 goats starting at 3 weeks postoperatively and was maintained until the time of euthanasia.

In 3 out of 4 goats, focal areas of markedly increased T_2 relaxation times (raw data provided in Table 2) were identified distal to the surgical incision in the epiphyseal cartilage during the first *in vivo* MRI session performed 3 weeks postoperatively (Figure 1) and remained apparent in the next imaging session at 6 weeks postoperatively (Figure 2 and Table 2). T_2 relaxation times in the corresponding areas in the contralateral, unoperated MFC remained low at 3 and 6 weeks postoperatively (Table 2). In the remaining goat (1/4), in which mean T_2 relaxation times in the operated MFC appeared identical to the contralateral, unoperated MFC, (36.22 ms vs. 36.57 ms and 40.86 ms vs. 41.07 ms at 3 and 6 weeks postoperatively [Table 2]) results of post mortem histological evaluation, performed immediately after the 6 week postoperative *in vivo* MRI session, were consistent with failure of surgical induction of ischemic cartilage necrosis (Figure 2). The AECC showed no histologically apparent lesions in this goat, consistent with the negative *in vivo* MRI results.

At 9 weeks postoperatively, all three remaining animals had an increased relaxation time in the operated area in the T_2 maps when compared to the contralateral limb (Table 2). In one of these animals, this lesion was accompanied by a pronounced delay in the progression of the ossification front (OC manifesta). This latter goat was euthanized 10 weeks postoperatively, and the presence of the above identified lesions was confirmed in the T_2 and adiabatic $T_{1\rho}$ maps obtained *ex vivo* at 9.4 Tesla. Subsequent histological evaluation of the operated medial femoral condyle in this goat demonstrated an extensive area of cartilage necrosis characterized by chondrocyte cell death in H&E-stained sections, pallor of the matrix in safranin O-stained sections, and delayed progression of the ossification front closely matching the findings of the *in vivo* MRI results (Figure 3).

A focal increase in the T_2 relaxation time (Table 2) along with mild (Figure 4) to marked (Figure 5) delay in the progression of the ossification front in the operated area were apparent in both goats examined 11 weeks postoperatively. In the contralateral limb T_2 relaxation times (Table 2) remained unchanged. Proton density images obtained from the

goat with the marked delay in the ossification front were also suggestive of the presence of a cleft involving the AECC in the operated area (Figure 4). T_2 and adiabatic $T_{1\rho}$ maps obtained *ex vivo* at 9.4 Tesla confirmed the presence of necrotic cartilage and mild (n=1) to marked (n=1) delay in progression of the ossification in each case. Results of the *in vivo* MRI studies were further confirmed by histological findings, including the presence of a cartilaginous flap (OC dissecans) as suspected from the proton density images (Figure 5).

Discussion

In the study reported here, surgical interruption of the vascular supply resulted in focal, ischemic necrosis of the AECC in 3 out of 4 operated goats. This focal area of ischemic chondronecrosis was successfully identified in all 3 affected goats at 3 weeks after surgery by using *in vivo* T_2 maps at 3 Tesla. A controlled exercise regimen likely was important in causing the progression to OCD of one of these lesions by 11 weeks after surgery, as previous studies in this model that did not include exercise did not result in the development of OCD (21). It is unclear why one goat failed to develop a lesion of ischemic necrosis, although this is most likely due to surgical error.

Previously, proof-of-principle studies aiming to confirm the importance of ischemic cartilage necrosis during the development of OC/OCD were successful both in pigs (5; 8) and horses (6). OC latens and OC manifesta lesions were induced in two different studies in pigs (5; 8), but development of clinically apparent OCD was not detected in either study, likely because of the relatively short follow up periods of 24 and 29 days. Conversely, an extended follow up period (49 days) that included access to pasture (unrestricted exercise) used in horses undergoing surgery to interrupt the vascular supply to a portion of the AECC of the lateral trochlear ridge of the distal femur enabled development of a clinically apparent OCD lesion by 42 days post operatively in one of the operated animals (6). Although these studies confirmed the role of vascular failure in the development of OC/OCD in animals, the species used are not ideally suited to serve as models of human OC/OCD, primarily because of their size, cost, and the fact that both pigs and horses have a relatively high incidence of naturally occurring OCD. To address these shortcomings, we attempted to induce OC/OCD in juvenile goats in a previous study using surgical interruption of the vascular supply to the epiphyseal cartilage of the axial portion of the medial femoral condyle, and by doing so create a clinically relevant animal model of human OC/OCD (21). Because the epiphysis in goats develops extremely rapidly (epiphyseal cartilage nearly completely replaced by bone by 11–12 weeks of age), the surgical procedures had to be performed on goats at the age of 5 days or younger. This ensured that a sufficient amount of vascularized epiphyseal cartilage was present at the time of surgery. Although we had a high success rate of inducing OC latens and OC manifesta lesions, none of the operated goats developed OCD in that study in spite of the prolonged (70 days) follow up period. (In sharp contrast to goats, the process of ossification in human beings occurs over a period of up to 10–12 years.) Hence, in our current work, based on the suspected role played by trauma in the development of OCD (12; 23; 24), we introduced an exercise-training program beginning 3 weeks after surgery to facilitate progression from OC manifesta to OCD. Relying on our previous study as a historical control, it is highly likely that progression of the induced lesion from OC latens through OC manifesta to OCD in one of the goats in the present study was facilitated by this

exercise training program, further corroborating the suspected role of biomechanical stress in the progression of OC manifesta to OCD. Nonetheless, the success rate of inducing an OCD lesion in 1 out of 4 goats remains low. This is most likely due to the relatively small volume of ischemic chondronecrosis developing after the surgical procedure as demonstrated by our histological and imaging results. In future studies, therefore, we propose to utilize a more extensive vascular interruption in combination with a post-operative exercise regimen.

During our previous studies, utilizing surgically induced OC latens and OC manifesta lesions in goats, we evaluated the ability of various MRI sequences to detect changes developing at various time points (16; 21). In these studies, lesions of ischemic chondronecrosis were identified as early as 2 weeks postoperatively with multiple sequences; however, the results were obtained *ex vivo* in a 9.4 Tesla MRI scanner using sequences that are not widely available, limiting the clinical utility of the results. Therefore, in the present study, the imaging procedures were performed in a 3 Tesla MRI scanner using clinically available sequences. Our results provide clear evidence that T_2 cartilage maps obtained *in vivo* at a clinically relevant field strength have the ability to identify areas of ischemic cartilage necrosis, thus providing a non-invasive approach to study OC/OCD during the early, subclinical stage of the disease. It is interesting to note, however, that the presence of the cartilage flap in goat 4, euthanized 11 weeks postoperatively, was only suspected in the PD weighted FSE sequence and not in the T_2 maps. The most likely explanation for this finding is that in the T_2 maps both necrotic cartilage and (synovial) fluid are characterized by markedly increased relaxation time, and therefore if they are superimposed over each other they are difficult to distinguish. Alternatively, T_2 maps obtained in selected regions as individual slices might just have missed the fissure if it happened to be between slices.

Prolonged imaging time is an important limitation associated with T_2 mapping which should be addressed before routine clinical implementation. To shorten the scan time, future studies may implement parallel acquisition methods, such as GRAPPA or SENSE techniques (25; 26). Further acceleration of the imaging process might be achieved by using multiband RF pulses as shown in diffusion MRI for functional brain studies (27). In spite of their demonstrated *ex vivo* utility in the diagnosis of subclinical OC lesions(16; 19), *in vivo* evaluation of susceptibility weighted imaging, RAFF and $T_{1\rho}$ sequences were not included in this study because of imaging time restrictions and/or their limited availability on clinical magnets.

Importantly, the present work provides the first solid proof for the purported progression from OC latens via OC manifesta to OCD in an individual subject, complementing the findings of Olstad *et al.* (28) who used sequential *in vivo* computed tomography in pigs to demonstrate progression and resolution of OC manifesta lesions. MRI studies using T_1, T_2 and proton density weighted imaging in a 1.5 Tesla magnet have already been performed in juvenile human subjects with the aim of better understanding the pathogenesis of OC/OCD (10; 11). In these studies, the authors distinguish ossification variants (irregularities of the ossification front) of the femoral condyles, which they consider normal, from lesions of OCD. Interestingly, lesions described as ossification variants, show a striking resemblance to

subclinical OC manifesta lesions described in animals using computed tomography and subsequently confirmed by histology (28). Furthermore, the authors of the human study note that “ossification variants can become symptomatic when repetitive stress is applied” (10). This latter observation appears to be consistent with the known ability of subclinical OC manifesta lesions in animals to undergo healing or progress to clinical disease (2; 28). T_2 cartilage maps now appear to lend a widely available approach to confirm whether ossification variants correspond with ischemic necrosis of the epiphyseal cartilage (termed OC latens and OC manifesta in the veterinary medical field) or are unrelated normal variants. Indeed, T_2 maps have already been successfully applied to evaluate healing after implantation of bone marrow-derived cells into cartilage defects in the femorotibial joints of human patients afflicted with OCD (15).

Potential weaknesses of the study include the low number of goats that were enrolled, although this led to an extremely efficient use of animals, which entailed completion of repeated imaging sessions in each goats at predetermined intervals as well as a highly labor-intensive daily exercise regimen. Acquisition of multiple sets of images from individual goats at different time points not only allowed monitoring of temporal progression of individual lesions, but also helped to diminish the negative effects of low animal numbers. Due to the low number of animals, however, we were unable to histologically confirm the lesions identified in the MRI studies 3 and 6 weeks post operatively. The close association of these lesions with the surgical incision, their consistent location in subsequent scans, their resemblance to the *ex vivo* findings from our previous study, and the lack of histological changes in the case which also provided negative MRI findings strongly indicate, however, that lesions noted in the MRI during the first 2 examinations are, indeed, areas of ischemic cartilage necrosis (OC latens). Unfortunately, neither conventional radiographs nor CT images were acquired at the time of MRI. Thus, no comparisons with MRI could be performed to contrast the ability of these methodologies to detect OC lesions in various stages of their development.

Because there is up to a 30% incidence of bilateral occurrence of OC/OCD of the knee (23), we propose MRI evaluation of the asymptomatic knee of future patients presented for (suspected) OC/OCD using T_2 maps. Identifying lesions of necrotic cartilage in these asymptomatic knees will not only provide early diagnosis, and by doing so afford a better opportunity for non-surgical management (3; 23), but will also facilitate a better understanding of the pathogenesis of OC/OCD in humans.

Acknowledgments

Support from NIH grants T32OD010993, K18OD010468, R21AR065385, K01 OD021293 was used during the completion of the study.

The authors are grateful to Drs. Mary Lauren Mesich and Elizabeth Pluhar for their assistance with the surgical procedures; to Kimberly Colvard, Lindsey Harper, Elizabeth Marchant and Melissa Roy for their help with the exercise training of the goats; and to Paula Overn for preparation of the histological sections.

References

1. McCoy AM, Toth F, Dolvik NI, et al. Articular osteochondrosis: a comparison of naturally-occurring human and animal disease. Osteoarthritis and cartilage/OARS, Osteoarthritis Research Society. 2013; 21:1638–1647.
2. Ytrehus B, Carlson CS, Ekman S. Etiology and pathogenesis of osteochondrosis. Veterinary pathology. 2007; 44:429–448. [PubMed: 17606505]
3. Cahill BR. Osteochondritis Dissecans of the Knee: Treatment of Juvenile and Adult Forms. The Journal of the American Academy of Orthopaedic Surgeons. 1995; 3:237–247. [PubMed: 10795030]
4. Kocher MS, Czarnecki JJ, Andersen JS, Micheli LJ. Internal fixation of juvenile osteochondritis dissecans lesions of the knee. Am J Sports Med. 2007; 35:712–718. [PubMed: 17337729]
5. Carlson CS, Meuten DJ, Richardson DC. Ischemic necrosis of cartilage in spontaneous and experimental lesions of osteochondrosis. Journal of orthopaedic research: official publication of the Orthopaedic Research Society. 1991; 9:317–329. [PubMed: 2010836]
6. Olstad K, Hendrickson EH, Carlson CS, et al. Transection of vessels in epiphyseal cartilage canals leads to osteochondrosis and osteochondrosis dissecans in the femoro-patellar joint of foals; a potential model of juvenile osteochondritis dissecans. Osteoarthritis and cartilage/OARS, Osteoarthritis Research Society. 2013; 21:730–738.
7. Olstad K, Ytrehus B, Ekman S, et al. Early lesions of osteochondrosis in the distal tibia of foals. Journal of orthopaedic research: official publication of the Orthopaedic Research Society. 2007; 25:1094–1105. [PubMed: 17415757]
8. Ytrehus B, Andreas Haga H, Mellum CN, et al. Experimental ischemia of porcine growth cartilage produces lesions of osteochondrosis. Journal of orthopaedic research: official publication of the Orthopaedic Research Society. 2004; 22:1201–1209. [PubMed: 15475198]
9. Carlson CS, Hilley HD, Meuten DJ. Degeneration of cartilage canal vessels associated with lesions of osteochondrosis in swine. Veterinary pathology. 1989; 26:47–54. [PubMed: 2913703]
10. Jans L, Jaremko J, Ditchfield M, et al. Ossification variants of the femoral condyles are not associated with osteochondritis dissecans. Eur J Radiol. 2012; 81:3384–3389. [PubMed: 22297186]
11. Jans LB, Jaremko JL, Ditchfield M, et al. MRI differentiates femoral condylar ossification evolution from osteochondritis dissecans. A new sign. Eur Radiol. 2011; 21:1170–1179. [PubMed: 21267576]
12. Edmonds EW, Polousky J. A review of knowledge in osteochondritis dissecans: 123 years of minimal evolution from Konig to the ROCK study group. Clinical orthopaedics and related research. 2013; 471:1118–1126. [PubMed: 22362466]
13. Ellermann J, Ling W, Nissi MJ, et al. MRI rotating frame relaxation measurements for articular cartilage assessment. Magnetic resonance imaging. 2013; 31:1537–1543. [PubMed: 23993794]
14. Rautiainen J, Lehto LJ, Tiitu V, et al. Osteochondral repair: evaluation with sweep imaging with fourier transform in an equine model. Radiology. 2013; 269:113–121. [PubMed: 23674789]
15. Vannini F, Battaglia M, Buda R, et al. "One step" treatment of juvenile osteochondritis dissecans in the knee: clinical results and T2 mapping characterization. Orthop Clin North Am. 2012; 43:237–244. vi. [PubMed: 22480472]
16. Wang L, Nissi MJ, Toth F, et al. Multiparametric MRI of Epiphyseal Cartilage Necrosis (Osteochondrosis) with Histological Validation in a Goat Model. PLoS One. 2015; 10:e0140400. [PubMed: 26473611]
17. Nissi, MJ., Toth, F., Carlson, CS., Ellermann, J. Intl Soc Mag Reson Med. Milan, Italy: 2014. Improved visualization of cartilage canals using semi-quantitative susceptibility mapping; p. 3986
18. Nissi MJ, Toth F, Zhang J, et al. Susceptibility weighted imaging of cartilage canals in porcine epiphyseal growth cartilage ex vivo and in vivo. Magnetic resonance in medicine: official journal of the Society of Magnetic Resonance in Medicine/Society of Magnetic Resonance in Medicine. 2014; 71:2197–2205.

19. Martel G, Kiss S, Gilbert G, et al. Differences in the vascular tree of the femoral trochlear growth cartilage at osteochondrosis-susceptible sites in foals revealed by SWI 3T MRI. Journal of orthopaedic research: official publication of the Orthopaedic Research Society. 2016
20. Toth F, Nissi MJ, Ellermann JM, et al. Novel Application of Magnetic Resonance Imaging Demonstrates Characteristic Differences in Vasculature at Predilection Sites of Osteochondritis Dissecans. Am J Sports Med. 2015
21. Toth F, Nissi MJ, Wang L, et al. Surgical induction, histological evaluation, and MRI identification of cartilage necrosis in the distal femur in goats to model early lesions of osteochondrosis. Osteoarthritis and cartilage/OARS, Osteoarthritis Research Society. 2015; 23:300–307.
22. Wang L, Nissi MJ, Toth F, et al. Quantitative susceptibility mapping detects abnormalities in cartilage canals in a goat model of preclinical osteochondritis dissecans. Magnetic resonance in medicine: official journal of the Society of Magnetic Resonance in Medicine/Society of Magnetic Resonance in Medicine. 2016
23. Crawford DC, Safran MR. Osteochondritis dissecans of the knee. The Journal of the American Academy of Orthopaedic Surgeons. 2006; 14:90–100. [PubMed: 16467184]
24. Nakano T, Aherne FX. Involvement of trauma in the pathogenesis of osteochondritis dissecans in swine. Can J Vet Res. 1988; 52:154–155. [PubMed: 3349396]
25. Pruessmann KP, Weiger M, Scheidegger MB, Boesiger P. SENSE: sensitivity encoding for fast MRI. Magnetic resonance in medicine: official journal of the Society of Magnetic Resonance in Medicine/Society of Magnetic Resonance in Medicine. 1999; 42:952–962.
26. Griswold MA, Jakob PM, Heidemann RM, et al. Generalized autocalibrating partially parallel acquisitions (GRAPPA). Magnetic resonance in medicine: official journal of the Society of Magnetic Resonance in Medicine/Society of Magnetic Resonance in Medicine. 2002; 47:1202–1210.
27. Barth M, Breuer F, Koopmans PJ, et al. Simultaneous multislice (SMS) imaging techniques. Magnetic resonance in medicine: official journal of the Society of Magnetic Resonance in Medicine/Society of Magnetic Resonance in Medicine. 2016; 75:63–81.
28. Olstad K, Kongsro J, Grindflek E, Dolvik NI. Ossification defects detected in CT scans represent early osteochondrosis in the distal femur of piglets. Journal of orthopaedic research: official publication of the Orthopaedic Research Society. 2014; 32:1014–1023. [PubMed: 24740876]

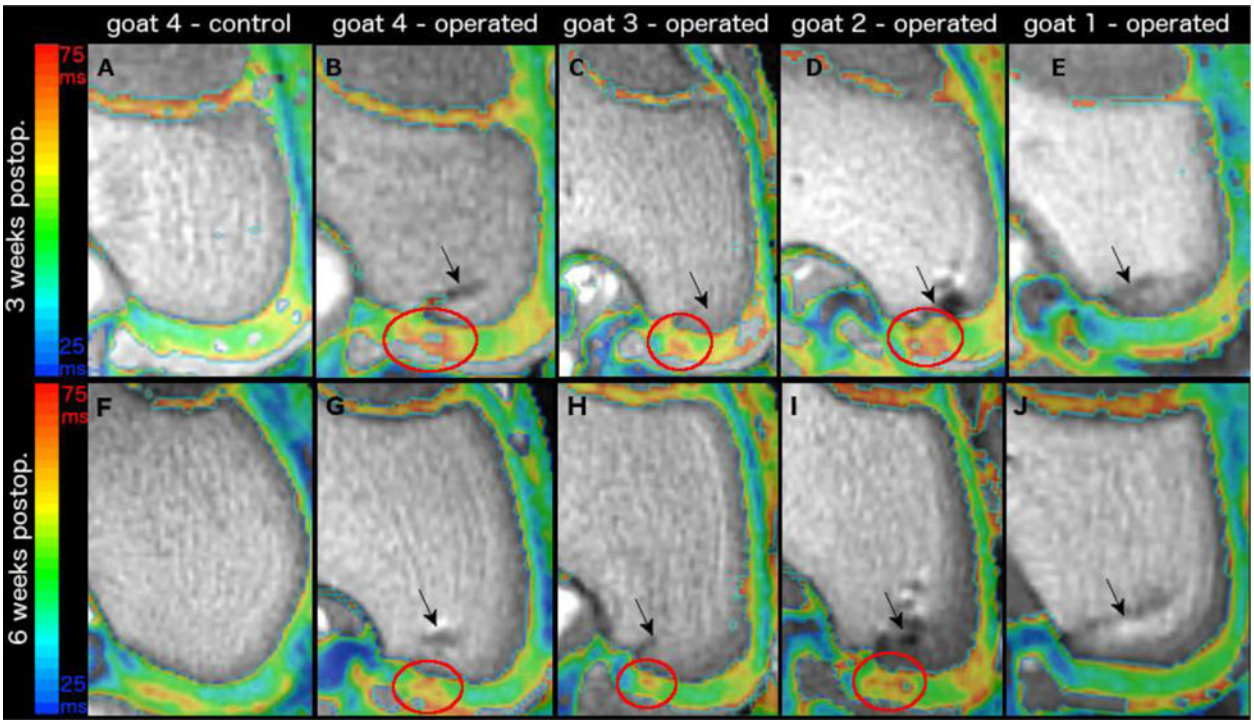

Figure 1.

depicts color T_2 maps (beneath which is the reference gray scale image generated from the shortest echo image of the T_2 mapping sequence) obtained *in vivo* in a 3T MR scanner in the coronal plane 3 weeks (first row) and 6 weeks (second row) after vascular interruption surgery in four goats. Panels A and F demonstrates normal epiphyseal cartilage of the medial femoral condyle in the left unoperated (control) limb of goat 4. Red ovals mark areas of increased relaxation time, consistent with ischemic cartilage necrosis, in the operated right medial femoral condyle of goats 4 (panels B and G), 3 (panels C and H), and 2 (Panels D and I). The epiphyseal cartilage appears normal in goat 1 (Panel E and J) where surgical interruption of the vascular supply to the medial femoral condyle failed. Black arrows indicate the surgical scars (Panels B–E and G–J).

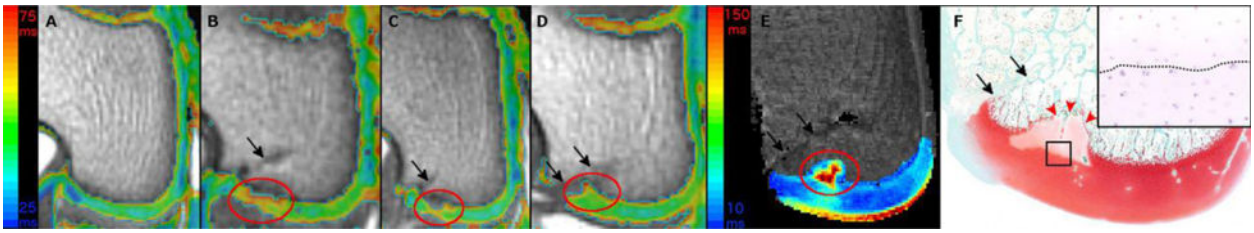

Figure 2.

depicts color T_2 maps (beneath which is the reference gray scale image generated from the shortest echo image of the T_2 mapping sequence) obtained *in vivo* in a 3T MR scanner in the coronal plane 9 weeks after vascular interruption surgery in three goats (Panels A–D). Panel A demonstrates normal epiphyseal cartilage of the medial femoral condyle in the left unoperated (control) limb of goat 4. Red ovals mark areas of increased relaxation time, consistent with ischemic cartilage necrosis, and delay of the progression of the ossification front (Panel D) in the operated right medial femoral condyle of goats 4, 3, and 2 (Panels B, C and D). Increased relaxation time and delayed progression of the ossification front in the area of ischemic cartilage necrosis (marked with red oval) are apparent in the T_2 map obtained at 9.4T *ex vivo* in goat 2 (Panel E). An area of ischemic chondronecrosis, characterized by pallor of the matrix is present in a safranin O stained histological section of the operated right medial femoral condyle of goat 2, and is accompanied by focal delay in the progression of the ossification front (red arrowheads, Panel F). Hematoxylin and eosin stained section at 40 × (inset) showing the interface of necrotic (above dotted line) and viable (below dotted line) epiphyseal cartilage from the area identified with the black rectangle in panel F. Black arrows indicate the surgical scars (Panels B–F).

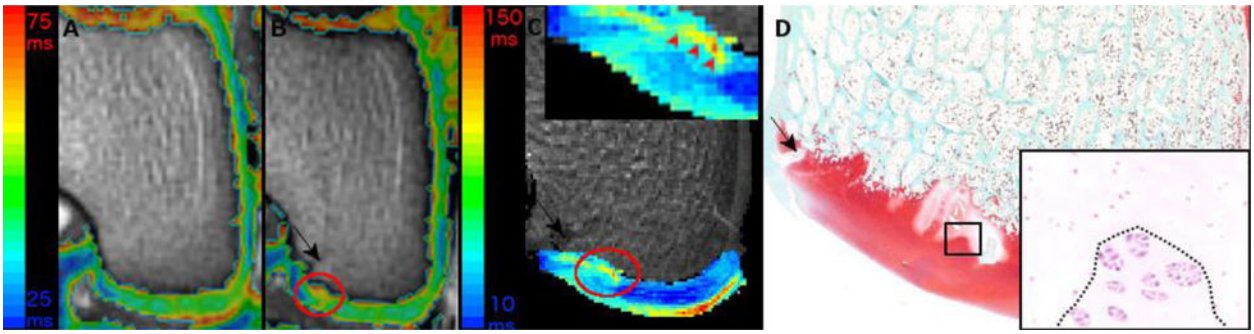

Figure 3.

depicts color T_2 maps (beneath which is the reference gray scale image generated from the shortest echo image of the T_2 mapping sequence) obtained *in vivo* in a 3T MR scanner in the coronal plane 11 weeks after vascular interruption surgery in goat 3 (Panels A and B). Panel A demonstrates normal epiphyseal cartilage of the medial femoral condyle in the left unoperated (control) limb. Red oval marks an area of increased relaxation time, consistent with ischemic cartilage necrosis, and a mild delay in the progression of the ossification front in the operated right medial femoral condyle (Panel B). Increased relaxation time and mild delay in the progression of the ossification front (inset, red arrowheads) in the area of ischemic cartilage necrosis are apparent in the T_2 map obtained at 9.4T *ex vivo* of the same goat (Panel C). Areas of ischemic chondronecrosis are marked by pallor in safranin O stained histological section of the operated right medial femoral condyle (Panel D). Hematoxylin and eosin stained section at 40 × (inset) showing the interface of necrotic (above dotted line) and viable (below dotted line) epiphyseal cartilage from the area identified with the black rectangle in panel D. Black arrows indicate the surgical scars (Panels B–D).

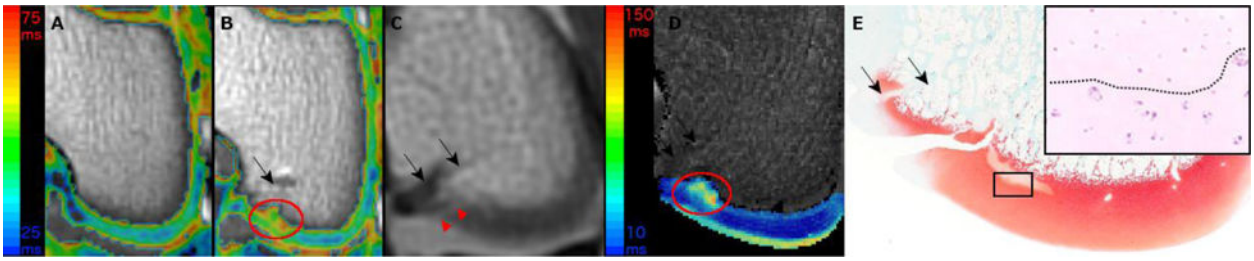

Figure 4.

depicts color T_2 maps (beneath which is the reference gray scale image generated from the shortest echo image of the T_2 mapping sequence) obtained *in vivo* in a 3T MR scanner in the coronal plane 11 weeks after vascular interruption surgery in goat 4 (Panels A and B). Panel A demonstrates normal epiphyseal cartilage of the medial femoral condyle in the left unoperated (control) limb. Red oval marks an area of increased relaxation time, consistent with ischemic cartilage necrosis, and delay of the progression of the ossification front in the operated right medial femoral condyle (Panel B). In the proton density image of the same goat, obtained *in vivo* at 3T, a faint linear hyperintensity (red arrowheads) is suggestive for a fissure extending through the articular-epiphyseal cartilage complex (Panel C). Increased relaxation time and delayed progression of the ossification front in the area of ischemic cartilage necrosis are apparent in the T2 map obtained at 9.4T *ex vivo* (Panel D). A fissure extending through the articular-epiphyseal cartilage complex is apparent in the safranin O stained histological section of the operated right medial femoral condyle (Panel E) along with an adjacent area of pallor consistent with cartilage necrosis. Hematoxylin and eosin stained section at 40 × (inset) showing the interface of necrotic (above dotted line) and viable (below dotted line) epiphyseal cartilage from the area identified with the black rectangle in panel E. Black arrows indicate the surgical scars (Panels B–E).

Table 1

Listing of all procedures undergone by individual goats

		Goat 1	Goat 2	Goat 3	Goat 4
In vivo MRI (3T)	3 weeks	completed	completed	completed	completed
	6 weeks	completed	completed	completed	completed
	9 weeks	Ø	completed	completed	completed
	11 weeks	Ø	Ø	completed	completed
Ex vivo MRI (9.4T)	10 weeks	Ø	completed	Ø	Ø
	11 weeks	Ø	Ø	completed	completed
Euthanasia @		6 weeks	10 weeks	11 weeks	11 weeks
Histology		completed	completed	completed	completed

Table 2

Mean ± SD of T_2 relaxation times [ms] for individual regions of interest drawn around areas of ischemic epiphyseal cartilage necrosis in the operated limb and around corresponding areas of (normal) epiphyseal cartilage in the control limbs for each goat and time point.

		T_2 relaxation times (mean ± SD [ms])			
		Week 3	**Week 6**	**Week 9**	**Week 11**
Goat 1*	**operated**	36.2±3.1*	40.9±4.2*		
	control	36.6±4.3*	41.1±4.6*		
Goat 2	**operated**	71.2±9.2	60.4±5.5	86.4±22	
	control	39.7±3.7	39.4±3.9	37.6±3.8	
Goat 3	**operated**	65.8±6.5	64.5±6.7	80.7±16.9	74.7±15.7
	control	38.3±4.8	39.4±4.9	39.9±3.7	36.3±6.6
Goat 4	**operated**	64.8±6.5	72.4±16.2	84.5±22.7	80.0±21.5
	control	41.2±4.2	40.6±3.0	40.0±5.4	42.6±4.7

• The surgical procedure failed to induce ischemic epiphyseal cartilage necrosis in goat 1.